Steel and Composite Structures, *Vol. 23, No. 3 (2017) 331-338*
DOI: https://doi.org/10.12989/scs.2017.23.3.331

Distortional buckling of cold-formed lipped channel columns subjected to axial compression

Wangbao Zhou [1,2a] and Lizhong Jiang [*1,2]

[1] *School of Civil Engineering, Central South University, Changsha 410075, China*
[2] *National Engineering Laboratory for High Speed Railway Construction, Changsha 410075, China*

(*Received July 16, 2016, Revised December 23, 2016, Accepted January 10, 2017*)

Abstract. Cold-formed lipped channel columns (CFLCCs) have been widely used in light gauge steel constructions. The distortional buckling is one of the important buckling modes for CFLCCs and the distortional buckling critical load depends significantly on the rotational restrain stiffness generated by the web to the lipped flange. First, a simplified explicit expression for the rotational restraint stiffness of the lipped flange has been derived. Using the expression, the characteristics of the rotational restraint stiffness of the lipped flange have been investigated. The results show that there is a linear coupling relationship between the applied forces and the rotational restraint stiffness of the lipped flange. Based on the explicit expression of the rotational restraint stiffness of the lipped flange, a simplified analytical formula has been derived which can determine the elastic distortional buckling critical stress of the CFLCCs subjected to axial compression. The simplified analytical formula developed in this study has been shown to be accurate through the comparisons with results from the distortional buckling analyses using the ANSYS finite element software. The developed analytical formula is easy to apply, and can be used directly in practical design and incorporated into future design codes and guidelines.

Keywords: cold-formed steel; lipped channel sections; rotational restraint stiffness; distortional buckling; axial compression

1. Introduction

Cold-formed lipped channel columns (CFLCCs) have been widely used in light gauge steel constructions because of its excellent comprehensive performance (Dar and Yusuf *et al*. 2015). Under axial compression, these CFLCCs may buckle in one of the several modes, such as the local buckling, distortional buckling, and flexural-torsional buckling (Lau and Hancock 1987, Hancock *et al*. 1994, Teng *et al*. 2003, He and Zhou 2014), as shown in Fig. 1. The distortional buckling, also known as the "stiffener buckling" or "local torsional buckling", is a mode characterized by the flexural-torsional buckling of the lipped flange elastically restrained by the web (Silvestre and Camotim 2010, Zhou *et al*. 2015b). Since the distortional buckling mode has been found to govern the strength of many cold-formed thin sections, it has received a great deal of attention and widespread concern from researchers over the last 20 years (He and Zhou 2014). During this period, many experimental and theoretical studies have been carried out on this mode of failure (Kwon and Hancock 1992, Hancock 1997, Kesti and Davies 1999, Silvestre and Camotim 2004, Silvestre *et al*. 2009, Landesmann and Camotim 2013, Young *et al*. 2013, Kwon *et al*. 2014, Niu *et al*. 2014a, Zhou *et al*. 2015b, Landesmann and Camotim 2016).

In the earlier studies, the distortional buckling critical stress was usually determined by a spline finite strip elastic buckling analysis (Kwon and Hancock 1992, Hancock *et al*. 1994). More recently, it was obtained using the user-friendly computer programs, such as: THIN-WALL (Papangelis and Hancock 1998), GBT (Silvestre and Camotim 2004), and CUFSM (Schafer 2012), ANSYS (Niu *et al*. 2014b, Shenggang *et al*. 2014). Unfortunately, the user is also often not familiar with the essentials of distortion. The analytical formulae for the distortional buckling critical stress calculation can unveil the distortional kinematics and mechanics of CFLCCs and provide definitions of cross-section properties that characterize the distortional mode (Silvestre and Camotim 2010). The design specifications (e.g., AS/NZS's (NAS 2007) and AISI's (AS/NZS 1996)) still require the distortional buckling critical load to be manually calculated using the analytical formulae because these formulae are popular design aids as they are considered most efficient (Silvestre and Camotim 2004, Zhou *et al*. 2015b). The analytical formulae for determining the distortional buckling critical stress of CFLCCs subjected to axial compression was first derived by Lau and Hancock (1987). The Lau and Hancock's solution has been included in the Australian/New Zealand standard (AS/NZS 1996) for the cold-formed steel structures because it is a simple method for determining the distortional buckling critical stress and is superior to the other methods. A modification to Lau and Hancock's formulae was further presented in Hancock

*Corresponding author, Ph.D.,
E-mail: lzhjiang@csu.edu.cn
[a] Ph.D., E-mail: zhouwangbao@163.com

ISSN: 1229-9367 (Print), 1598-6233 (Online)

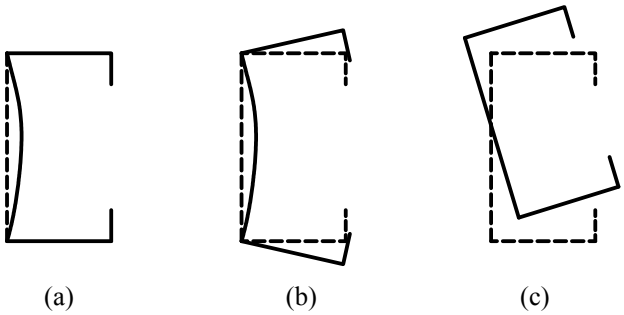

(a) (b) (c)

Fig. 1 Buckling modes (a) local buckling; (b) distortional buckling; (c) flexural-torsional buckling

(1997), which can be used to determine the distortional buckling strength of a flexural member. An extension of Lau and Hancock's formula for beam-columns with biaxial bending was further presented in Teng *et al*. (2003). Li and Chen (2008) also presented a closed-form solution for the distortional buckling strength of the cold-formed steel sections using a similar model developed by Lau and Hancock (1987). Based on the generalised beam theory, Silvestre and Camotim (2004) derived a set of formula which can estimate the distortional buckling critical load of CFLCCs (Silvestre and Camotim 2004). The accuracy and range of validity for the derived formula was validated in (Silvestre and Camotim 2004). Lau and Hancock (1987) re-derived the explicit expression for the rotational restraint stiffness provided by the web on the lipped flange, and the coupling effect between the applied forces and the torsional restraint stiffness of the lipped flange was shown in the expression. By carrying out a large number of numerical calculations of the rotational restraint stiffness, Teng and Yao *et al*. showed that the rotational restraint stiffness of the lipped flange varies approximately linearly with the compressive stress of the web (Teng *et al*. 2003). However, for the distortional critical buckling stress of CFLCCs, the Lau and Hancock' formula (1987) and the Teng and Yao' formula (Teng *et al*. 2003, Yao 2008) possess a number of limitations, namely:

(1) Lau and Hancock' formula (1987) requires the tedious repetitive iterations in order to obtain the distortional buckling critical load of CFLCCs because of using very complex formulae for the rotational restraint stiffness.
(2) Teng *et al*. (2003) showed that the rotational restraint stiffness of the lipped flange varies approximately linearly with the compressive stress of the web by carrying out a large number of numerical calculations, but fail to develop the explicit expression of rotational restraint stiffness of the lipped flange, which makes calculation of distortional critical buckling stress very difficult and complicated.

This paper presents a simplified closed-form solution for the rotational restraint stiffness of the lipped flange of CFLCC subjected to axial compression. The solution is an extension of the Lau and Hancock's solution (Lau and Hancock 1987). The solution also shows that the theoretical

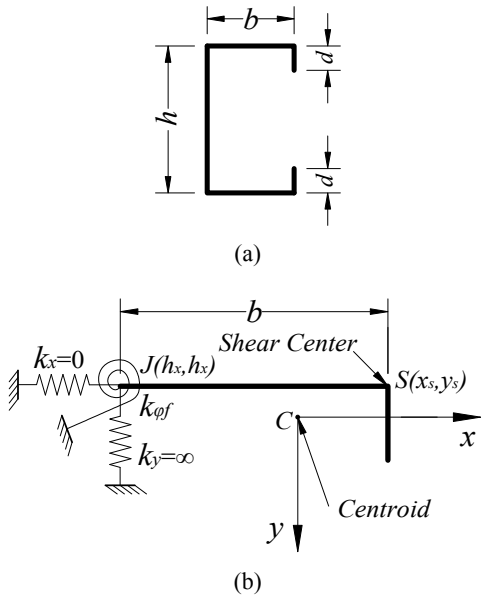

Fig. 2 Theoretical model for distortional buckling: (a) original section; (b) theoretical model

relationship between the applied forces and the torsional restraint stiffness of the lipped flange is linear, i.e. the rotational restraint stiffness of the lipped flange can be determined not only from the geometry and material characteristics of a CFLCC but also from the applied forces. Based on the closed-form solution of the rotational restraint stiffness developed in this study, a simplified analytical formula is further presented for the determination of the elastic distortional buckling critical stress of the CFLCCs subjected to axial compression. The validity of the simplified analytical formula has been verified numerically by comparing the results with the buckling analysis using the ANSYS finite element software. At the end of this paper, there is a simple design example showing the application of the analytical expression.

2. Basic assumptions

Since the distortional buckling mode mainly involves the lateral bending and rotation of the lipped flange about the web-flange junction, by assuming that they are rigid bodies, an approximate expression can be derived by considering the lipped flanges only (Lau and Hancock 1987, Hancock 1997, Schafer and Peköz 1999, Teng *et al*. 2003, Yu and Schafer 2006, Tong *et al*. 2015, Zhou *et al*. 2015b). Hence, the top lipped flange of the CFLCC in Fig. 2(a) have been isolated as shown in Fig. 2(b). The effects of the web on the top lipped flange have been modeled with a rotational spring, a lateral spring and a vertical spring, which restrain the deformation of the lipped flange. The stiffnesses of the three elastic springs are given by $k_{\varphi f}$, k_x and k_y, respectively. The coordinate axes have been chosen such that the x-axis is parallel to the flange, and the origin is at the centroid of the lipped flange. To simplify the calculation, the following assumptions have been made (Lau and Hancock 1987, Teng *et al*. 2003).

(1) Since the web is stiff in its own plane, it has been assumed that its in-plane stiffness $k_y = \infty$.

(2) Since the web's out of plane flexural rigidity is low, it has been assumed that its out-of-plane stiffness $k_x = 0$.

3. Simplified closed-form solution for rotational restraint stiffness

Fig. 3 shows a simplified theoretical model of a CFLCC web, in which the four edges of the web are simply supported. The two transversal edges of the web are subjected to uniform compressive stresses, in which if the stress is positive, it is compressive. Generated by the lipped flanges, the two longitudinal edges are subjected to distributed bending moments. Then, the boundary conditions of the web can be written as

$$\left[-D\left(\frac{\partial^2 w}{\partial y^2}+\mu\frac{\partial^2 w}{\partial z^2}\right)\right]_{y=0,h} = m(z) = -k_{\varphi w}\left[\frac{\partial w}{\partial y}\right]_{y=0,h} \tag{1}$$

$$[w]_{y=0,h} = 0, \qquad [w]_{z=0,\lambda} = 0, \qquad \left[\frac{\partial^2 w}{\partial z^2}\right]_{z=0,\lambda} = 0 \tag{2}$$

where $D = Et^3/[12(1-\mu^2)]$ is the plate flexural stiffness per unit width, μ is the Poisson's ratio, E is the elasticity modulus, t is the thickness of the web, w is the out-of-plane buckling deformation function of the web, h is the height of the web, $k_{\varphi f}$ is the rotational restrain stiffness provided by the web on the lipped flange, λ is the distortional buckling half-wavelength, which is equal to the CFLCC length divided by the number of buckling half-waves.

Given the above-mentioned boundary conditions, the buckling displacement function of the web can be approximated by a combination of two trigonometric functions with one unknown coefficients as follows

$$w = f\sin\frac{\pi y}{h}\sin\frac{\pi z}{\lambda} \tag{3}$$

where f is the general coordinate representing the amplitude of the distortional buckling deformation.

Using the finite strip buckling analysis program, Yao (2008) carried out a number of parametric studies in terms of the distortional buckling half-wavelength of the CFLCC (Yao 2008). He developed the following approximate

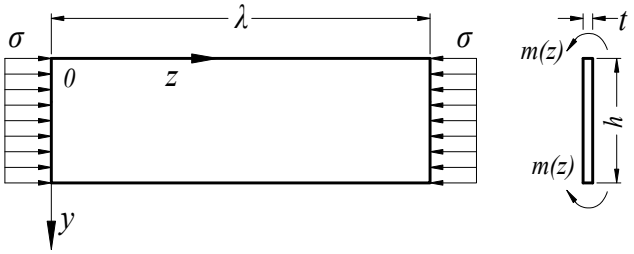

Fig. 3 Web subjected to compressive stresses and distributed moments

expression for the distortional buckling half-wavelength

$$\lambda_{cr} = 3.48b\left(\frac{h}{b}\right)^{0.15}\left(\frac{b}{t}\right)^{-0.2}\left(\frac{d}{t}\right)^{0.7} \tag{4}$$

where b and d are the widths of the flange and lip, respectively.

According to the tiny deflection theory of thin plates (Timoshenko and Gere 1961, Jiang *et al*. 2013, Tong *et al*. 2015), the bending strain energy of the web is

$$U_1 = \frac{D}{2}\int_0^{\lambda}\int_0^{h}\left[\left(\frac{\partial^2 w}{\partial y^2}\right)^2+\left(\frac{\partial^2 w}{\partial z^2}\right)^2\right. \tag{5}$$

$$\left.+2\mu\frac{\partial^2 w}{\partial y^2}\frac{\partial^2 w}{\partial z^2}+2(1-\mu)\left(\frac{\partial^2 w}{\partial y\partial z}\right)^2\right]\mathrm{dydz} \tag{5}$$

Substituting Eq. (3) into Eq. (5) gives

$$U_1 = \frac{Df^2\lambda h}{8}\left[\left(\frac{\pi}{h}\right)^2+\left(\frac{\pi}{\lambda}\right)^2\right]^2 \tag{6}$$

The deformation energy yielded by the rotational spring of the web is (Zhou *et al*. 2016a, b)

$$U_2 = \frac{k_{\varphi w}}{2}\int_0^{\lambda}\left\{\left[\frac{\partial w}{\partial y}\right]_{y=0}^2+\left[\frac{\partial w}{\partial y}\right]_{y=h}^2\right\}\mathrm{dz} \tag{7}$$

Substituting Eq. (3) into Eq. (7) gives

$$U_2 = \frac{k_{\varphi w}f^2\lambda}{2}\left(\frac{\pi}{h}\right)^2 \tag{8}$$

The external work of the web can be described by (Jiang *et al*. 2013)

$$W = \frac{t}{2}\int_0^{\lambda}\int_0^{h}\sigma\left(\frac{\partial w}{\partial z}\right)^2\mathrm{dydz} \tag{9}$$

Substituting Eq. (3) into Eq. (9) gives

$$W = \frac{f^2\lambda ht\sigma}{8}\left(\frac{\pi}{\lambda}\right)^2 \tag{10}$$

The total potential energy of the web can be given by (Jiang *et al*. 2013, Magnucki *et al*. 2014)

$$\Pi = U_1 + U_2 - W \tag{11}$$

Substituting Eqs. (6), (8) and (10) into Eq. (11) gives

$$\Pi = \frac{Df^2\lambda h}{8}\left[\left(\frac{\pi}{h}\right)^2+\left(\frac{\pi}{\lambda}\right)^2\right]^2+\frac{k_{\varphi w}f^2\lambda}{2}\left(\frac{\pi}{h}\right)^2-\frac{f^2\lambda ht\sigma}{8}\left(\frac{\pi}{\lambda}\right)^2 \tag{12}$$

Based on the principle of minimum potential energy (Jiang *et al*. 2013, Ye and Chen 2013, Benselama *et al*. 2015), the equation for rotational restraint stiffness is

$$\left\{\frac{D\lambda h}{4}\left[\left(\frac{\pi}{h}\right)^2+\left(\frac{\pi}{\lambda}\right)^2\right]^2+k_{\varphi w}\lambda\left(\frac{\pi}{h}\right)^2-\frac{\lambda ht\sigma}{4}\left(\frac{\pi}{\lambda}\right)^2\right\}f=0 \quad (13)$$

When there is distortional buckling in the CFLCC, the general coordinate f cannot be zero. Hence, equating the determinant of Eq. (13) to zero gives the following equation, which can be used to determine the rotational restraint stiffness of the web

$$\frac{Dh}{4}\left[\left(\frac{\pi}{h}\right)^2+\left(\frac{\pi}{\lambda}\right)^2\right]^2+k_{\varphi w}\left(\frac{\pi}{h}\right)^2-\frac{ht\sigma}{4}\left(\frac{\pi}{\lambda}\right)^2=0 \quad (14)$$

Solving Eq. (14) gives the following explicit expression for the rotational restraint stiffness of the web

$$k_{\varphi w}=\frac{ht\beta_2\sigma-Dh\left(\beta_1+\beta_2\right)^2}{4\beta_1} \quad (15)$$

where $\beta_1=\pi^2/h^2$, $\beta_2=\pi^2/\lambda^2$.

To include the effects of flange distortion and shear, the term D in Eq. (15) has been modified to D_w (Yao 2008), as follows

$$D_w=\frac{Dh}{h+a\lambda} \quad (16)$$

$$a=0.1\left(\frac{b}{d}\right)^{0.87}\left(\frac{b}{t}\right)^{-0.56}\left(1+0.3\frac{b}{h}\right) \quad (17)$$

The modified expression for the rotational restraint stiffness of web is

$$k_{\varphi w}^{'}=\frac{ht\beta_2\sigma-D_wh\left(\beta_1+\beta_2\right)^2}{4\beta_1} \quad (18)$$

The modified expression for the rotational restraint stiffness of web is

$$k_{\varphi f}=-k_{\varphi w}^{'}=\alpha_0-\alpha_1\sigma \quad (19)$$

$$\alpha_0=\frac{D_wh\left(\beta_1+\beta_2\right)^2}{4\beta_1},\qquad \alpha_1=\frac{ht\beta_2}{4\beta_1} \quad (20)$$

Teng *et al*. (2003) carried out a number of parametric studies for the rotational restraint stiffness of the lipped flange. They showed that the rotational restraint stiffness of the lipped flange varied approximately linearly with the applied forces. Eq. (19) is an extension of the Teng *et al*.'s (2003) solution, which proves that the theoretical coupling relationship between the applied force and the torsional restraint stiffness of the lipped flange is linear, i.e. the rotational restraint stiffness of the lipped flange can be determined not only from the geometry and material characteristics of a CFLCC but also from the applied forces. The formula (Eq. (19)) developed in this study has been further developed to a simple analytical formula in Section 4, which can be used in design to determine the distortional buckling critical stress of CFLCCs.

$$\sigma_0=\alpha_0/\alpha_1=\alpha_0=\frac{D_w\left(\beta_1+\beta_2\right)^2}{t\beta_2} \quad (21)$$

where σ_0 is the critical stress that govern whether the torsional restraint stiffness of the lipped flange is positive, zero or negative. The torsional restraint stiffness of the lipped flange is (1) positive when the applied stress $\sigma<\sigma_0$, (2) negative when the applied stress $\sigma>\sigma_0$, and (3) zero when the applied stress $\sigma=\sigma_0$.

4. Simplified closed-form solution for distortional buckling critical stiffness

4.1 Analytical formulations

The deflections for the shear center of the lipped flange section in the x and y directions are u and v, respectively, and the rotation of the lipped flange section about the shear center is the angel φ. By considering the equilibrium of moments about the shear center axis and the equilibrium of forces in the x and y directions, the distortional buckling critical load is governed by the following three simultaneous differential equations (Timoshenko and Gere 1961, Lau and Hancock 1987, Teng *et al*. 2003, Zhou *et al*. 2015a, Zhou *et al*. 2016a).

$$EI_y\frac{\mathrm{d}^4u}{\mathrm{d}z^4}+EI_{xy}\frac{\mathrm{d}^4v}{\mathrm{d}z^4}+P\frac{\mathrm{d}^2u}{\mathrm{d}z^2}+y_sP\frac{\mathrm{d}^2\varphi}{\mathrm{d}z^2}+k_x\left[u+\left(y_s-h_y\right)\varphi\right]=0 \quad (22)$$

$$EI_x\frac{\mathrm{d}^4v}{\mathrm{d}z^4}+EI_{xy}\frac{\mathrm{d}^4u}{\mathrm{d}z^4}+P\frac{\mathrm{d}^2v}{\mathrm{d}z^2}-x_sP\frac{\mathrm{d}^2\varphi}{\mathrm{d}z^2}+k_y\left[v-\left(x_s-h_x\right)\varphi\right]=0 \quad (23)$$

$$\begin{aligned}&EI_\omega\frac{\mathrm{d}^4\varphi}{\mathrm{d}z^4}-\left(GJ-r_s^2P\right)\frac{\mathrm{d}^2\varphi}{\mathrm{d}z^2}+y_sP\frac{\mathrm{d}^2u}{\mathrm{d}z^2}-x_sP\frac{\mathrm{d}^2v}{\mathrm{d}z^2}+k_{\varphi f}\varphi\\&+k_x\left[u+\left(y_s-h_y\right)\varphi\right]\left(y_s-h_y\right)-k_y\left[v-\left(x_s-h_x\right)\varphi\right]\left(x_s-h_x\right)=0\end{aligned} \quad (24)$$

$$r_s^2=\left(I_x+I_y\right)\Big/A+x_s^2+y_s^2 \quad (25)$$

where, as shown in Fig. 2, x_s and y_s are the x and y coordinates of the shear center of the lipped flange, respectively; h_x and h_y are the x and y coordinates of the web/flange junction, respectively; I_x, I_y and I_{xy} are the moment of inertias of the lipped flange section about the x and y axes and the product second moment of area, respectively; and J and I_ω are the torsional constant and warping constant of the lipped flange section, respectively. $P=\sigma A$ where A is the cross-sectional area of the lipped flange. G is the shear module, and r_s^2 is the polar second moment of area about the shear center.

With the assumption of $k_y=\infty$, at the support, there is no deformation in the y direction. Hence, the vertical deformation of the shear center is

$$v=\left(x_s-h_x\right)\varphi \quad (26)$$

The term $k_y\left[v-\left(x_s-h_s\right)\varphi\right]$ in Eqs. (23) and (24) can be replaced by the reaction R_y, which is the intensity of the distributed reaction force in the y direction provided by the

support. Therefore, Eqs. (23) and (24) can be re-written as

$$EI_x\left(x_s-h_x\right)\frac{\mathrm{d}^4\varphi}{\mathrm{d}z^4}+EI_{xy}\frac{\mathrm{d}^4u}{\mathrm{d}z^4}-h_xP\frac{\mathrm{d}^2\varphi}{\mathrm{d}z^2}+R_y=0 \tag{27}$$

$$\begin{aligned}&EI_\omega\frac{\mathrm{d}^4\varphi}{\mathrm{d}z^4}-\left(GJ-r_s^2P\right)\frac{\mathrm{d}^2\varphi}{\mathrm{d}z^2}+y_sP\frac{\mathrm{d}^2u}{\mathrm{d}z^2}-x_sP\left(x_s-h_x\right)\frac{\mathrm{d}^2\varphi}{\mathrm{d}z^2}+k_{\varphi f}\varphi\\&+k_x\left[u+\left(y_s-h_y\right)\varphi\right]\left(y_s-h_y\right)-R_y\left(x_s-h_x\right)=0\end{aligned} \tag{28}$$

With the assumption of $k_x = 0$, Eqs. (22) and (28) can be re-written as

$$EI_y\frac{\mathrm{d}^4u}{\mathrm{d}z^4}+EI_{xy}\left(x_s-h_x\right)\frac{\mathrm{d}^4\varphi}{\mathrm{d}z^4}+P\frac{\mathrm{d}^2u}{\mathrm{d}z^2}+y_sP\frac{\mathrm{d}^2\varphi}{\mathrm{d}z^2}=0 \tag{29}$$

$$\begin{aligned}&EI_\omega\frac{\mathrm{d}^4\varphi}{\mathrm{d}z^4}-\left(GJ-r_s^2P\right)\frac{\mathrm{d}^2\varphi}{\mathrm{d}z^2}+y_sP\frac{\mathrm{d}^2u}{\mathrm{d}z^2}\\&-x_sP\left(x_s-h_x\right)\frac{\mathrm{d}^2\varphi}{\mathrm{d}z^2}+k_{\varphi f}\varphi-R_y\left(x_s-h_x\right)=0\end{aligned} \tag{30}$$

$$\begin{aligned}&\left[EI_\omega+EI_x\left(x_s-h_x\right)^2\right]\frac{\mathrm{d}^4\varphi}{\mathrm{d}z^4}+EI_{xy}\left(x_s-h_x\right)\frac{\mathrm{d}^4u}{\mathrm{d}z^4}\\&+\left(r_j^2P-GJ\right)\frac{\mathrm{d}^2\varphi}{\mathrm{d}z^2}+y_sP\frac{\mathrm{d}^2u}{\mathrm{d}z^2}+k_{\varphi f}\varphi=0\end{aligned} \tag{31}$$

$$r_j^2=h_x^2-x_s^2+r_s^2=\left(I_x+I_y\right)/A+y_s^2+h_x^2 \tag{32}$$

4.2 Simplified expressions

The distortional buckling behavior of the lipped flange is now governed by Eqs. (29) and (30). Taking the solutions of Eqs. (29) and (30) in the form of

$$\varphi=C_1\sin\frac{\pi z}{\lambda},\qquad u=C_2\sin\frac{\pi z}{\lambda} \tag{33}$$

Substituting Eqs. (33) and (19) into Eqs. (29) and (31) gives

$$\left(\eta_1-y_sP\right)C_1+\left(\eta_2-P\right)C_2=0 \tag{34}$$

$$\left(\eta_3-\eta_4P\right)C_1+\left(\eta_1-y_sP\right)C_2=0 \tag{35}$$

$$\eta_1=EI_{xy}\left(x_s-h_x\right)\beta_2 \tag{36}$$

$$\eta_2=EI_y\beta_2 \tag{37}$$

$$\eta_3=EI_\omega\beta_2+EI_x\left(x_s-h_x\right)^2\beta_2+GJ+\alpha_0/\beta_2 \tag{38}$$

$$\eta_4=r_j^2+\alpha_1/\left(A\beta_2\right) \tag{39}$$

Equating the determinant of Eqs. (34) and (35) to zero gives the following quadratic equations

$$\left(\eta_1-y_sP\right)^2-\left(\eta_2-P\right)\left(\eta_3-\eta_4P\right)=0 \tag{40}$$

$$\left(y_s^2-\eta_4\right)P^2+\left(\eta_2\eta_4-2\eta_1y_s+\eta_3\right)P+\eta_1^2-\eta_2\eta_3=0 \tag{41}$$

Equating the determinant of Eqs. (40) and (41) to zero gives the following quadratic equations

$$\sigma_{\mathrm{cr}}=\min\left\{\frac{-\alpha_3-\sqrt{\alpha_3^2-4\alpha_2\alpha_4}}{2\alpha_2A},\frac{-\alpha_3+\sqrt{\alpha_3^2-4\alpha_2\alpha_4}}{2\alpha_2A}\right\} \tag{42}$$

$$\alpha_2=y_s^2-\eta_4 \tag{43}$$

$$\alpha_3=\eta_2\eta_4-2\eta_1y_s+\eta_3 \tag{44}$$

$$\alpha_4=\eta_1^2-\eta_2\eta_3 \tag{45}$$

Given that

$$\alpha_2=y_s^2-\eta_4=-h_x^2-\alpha_1/\left(A\beta_2\right)-\left(I_x+I_y\right)/A<0 \tag{46}$$

Then, the distortional buckling critical stress can be re-written as

$$\sigma_{\mathrm{cr}}=\frac{-\alpha_3+\sqrt{\alpha_3^2-4\alpha_2\alpha_4}}{2\alpha_2A} \tag{47}$$

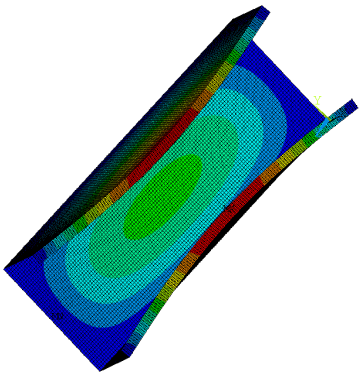

Fig. 4 Distortional buckling mode of a test member

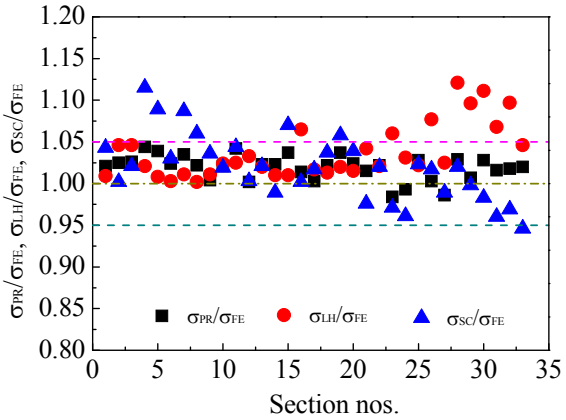

Fig. 5 Comparison of critical stress ratios determined from simplified formula (Eq. (47)), Lau and Hancock's (1987) formula, Silvestre and Camotim' formula (2010) and ANSYS finite elements analysis

Table 1 Comparison of distortional buckling loads

Section nos.	Section dimensions(mm)				Critical stress (MPa)				Critical stress ratios		
	h	*b*	*d*	*t*	σ_{FE}	σ_{PR}	σ_{LH}	σ_{SC}	σ_{PR}/σ_{FE}	σ_{LC}/σ_{FE}	σ_{SC}/σ_{FE}
C1	60	40	5	1.0	193.9	198.0	195.7	202.2	1.021	1.009	1.043
C2	60	30	5	1.5	477.1	489.0	499.2	478.3	1.025	1.046	1.002
C3	60	30	6	1.5	527.3	541.3	551.5	538.2	1.026	1.046	1.021
C4	60	60	6	1.0	116.2	121.4	118.7	129.6	1.044	1.021	1.115
C5	60	50	6	1.0	158.1	164.3	159.5	172.2	1.039	1.008	1.089
C6	60	40	6	1.0	222.9	228.1	223.6	229.5	1.024	1.003	1.030
C7	70	60	6	1.0	109.8	113.7	111.0	119.3	1.035	1.011	1.087
C8	70	50	6	1.0	147.6	150.8	147.9	156.5	1.022	1.002	1.060
C9	70	40	6	1.0	201.7	202.4	203.9	208.9	1.004	1.011	1.036
C10	70	40	6	1.5	337.8	344.9	346.0	344.2	1.021	1.024	1.019
C11	70	50	6	1.5	245.5	255.9	251.7	256.3	1.042	1.025	1.044
C12	80	40	6	1.5	304.9	305.4	314.9	305.9	1.002	1.033	1.003
C13	80	50	6	1.5	229.6	234.9	234.1	234.4	1.023	1.020	1.021
C14	80	50	8	1.5	281.5	287.8	284.3	278.4	1.023	1.010	0.989
C15	80	60	8	1.5	215.7	223.7	218.0	230.8	1.037	1.010	1.070
C16	90	40	7	2.0	436.7	442.9	464.9	437.7	1.014	1.065	1.002
C17	90	50	7	1.5	236.9	237.5	240.9	241.0	1.003	1.017	1.017
C18	90	60	7	1.5	184.0	188.0	186.3	190.8	1.022	1.013	1.037
C19	90	70	7	1.5	144.2	149.5	147.1	152.5	1.037	1.020	1.058
C20	100	70	7	1.5	137.5	140.9	139.5	142.9	1.024	1.015	1.039
C21	100	50	6	2.0	292.0	296.5	304.3	285.0	1.015	1.042	0.976
C22	100	60	8	2.0	276.4	282.5	282.3	282.0	1.022	1.021	1.020
C23	120	50	5	1.5	142.7	140.4	151.3	138.6	0.984	1.060	0.971
C24	120	60	5	1.5	120.2	119.3	123.9	115.5	0.993	1.031	0.961
C25	120	80	8	2.0	164.1	168.7	167.7	167.9	1.028	1.022	1.023
C26	140	60	8	2.0	200.2	200.9	215.7	203.7	1.003	1.077	1.017
C27	140	70	8	2.0	177.5	175.0	182.0	175.5	0.986	1.025	0.989
C28	140	50	8	2.5	305.7	314.5	342.8	311.8	1.029	1.121	1.020
C29	160	60	8	2.5	231.7	233.4	254.1	231.2	1.007	1.096	0.998
C30	160	60	8	3.0	304.4	312.9	338.3	299.2	1.028	1.111	0.983
C31	160	70	8	3.0	276.0	280.4	294.8	265.0	1.016	1.068	0.960
C32	180	70	8	3.0	236.8	241.1	259.7	229.3	1.018	1.097	0.969
C33	180	90	8	3.0	190.8	194.6	199.5	180.6	1.020	1.046	0.946
				Mean					1.019	1.037	1.019
				SD					0.015	0.033	0.040
				Max					1.044	1.121	1.115
				Min					0.984	1.002	0.946

5. Examples of analyses

In order to assess the accuracy of the developed calculation formula (Eq. (47)), both the simplified calculation method introduced in this paper and the finite element method have been used to determine the distortional buckling critical stresses of 33 test members subjected to axial compression. The geometrical dimensions of the 33 test members are shown in Table 1. The ANSYS commercial software has been used to carry out the finite element analysis of the distortional buckling mode of the 33 test members.

Fig. 4 shows the results of one selected member. The Young's modulus is 2.1×10^5 MPa, and the Poisson's ratio is 0.3. The CFLCC has been modeled using the 4-node, quadrilateral, shell 181 elements. The uniform compressive stresses acting at the two ends of the CFLCC have been translated into equivalent concentrated node loads, which act on the corresponding element nodes in the finite element analysis. The size of the element mesh is 1.5 mm or less in

order to meet the equivalent relationship between the equivalent concentrated node loads and the uniform compressive stress. The two degrees of freedom at the two ends of the CFLCC in the x and y directions have been restrained. Hence, the torsion at the two ends of the CFLCC has also been restrained. The degree of freedom of one node at the right end in the *z* direction has been restrained in order to meet the static balance requirements

To show the advantage of the proposed formula (Eq. (47)) in comparison with other available formulae and to assess the accuracy of the proposed formula, the Lau and Hancock' formula (1987) and Silvestre and Camotim' formulae (Silvestre and Camotim 2004, Silvestre and Camotim 2010) are compared with the formula (Eq. (47)) proposed in this study. Table 1 shows the critical distortional buckling stress obtained through (1) ANSYS commercial software, (2) the Lau and Hancock' formula (1987), (3) the Silvestre and Camotim' formulae (Silvestre and Camotim 2004, Silvestre and Camotim 2010), and (4) the proposed formula (Eq. (47)). Fig. 5 shows the variations of critical stress ratios σ_{PR}/σ_{FE}, σ_{LH}/σ_{FE} and σ_{SC}/σ_{FE} with the section numbers. The σ_{PR}, σ_{LH}, σ_{SC} and σ_{FE} are the stresses obtained from Eq. (47), Lau and Hancock' formula, Silvestre and Camotim' formulae and ANSYS finite element analysis, respectively. Observation of the results displayed in Fig. 5 and Table 1 led to the following conclusions assuming that the stresses determined by the ANSYS finite element method are accurate:

(1) The estimates provided by the proposed formula (Eq. (47)) exhibit errors never exceeding 5.0% (the max is 1.044 and the min is 0.984), while the estimates provided by the Lau and Hancock' formula(1987) and the Silvestre and Camotim' formula (Silvestre and Camotim 2004, Silvestre and Camotim 2010) exhibit errors reaching 12% (the max is 1.121 and the min is 1.002) and exceeding 11% (the max is 1.115 and the min is 0.946), respectively. This shows that more accurate estimates for the distortional buckling critical stress can be obtained by using the torsional restraint stiffness of the lipped flange developed in this study.

(2) For the proposed formula, the average and standard deviation values of σ_{PR}/σ_{FE} were 1.019 and 0.015, respectively, whereas they were 1.037 and 0.033, respectively, for the Lau and Hancock' formula (1987) and were 1.019 and 0.040, respectively, for the Silvestre and Camotim' formulae (Silvestre and Camotim 2004, Silvestre and Camotim 2010). This indicates that the proposed formula provides more accurate estimates for CFLCCs than the Lau and Hancock' formula (1987) and has similar accuracy with the Silvestre and Camotim' formulae (Silvestre and Camotim 2004, Silvestre and Camotim 2010).

In order to demonstrate the application of the developed formula (Eq. (47)) for calculating the distortional buckling critical stress, Section C17 in Table 1 has been selected as an example. In the application, the Young's modulus is 2.1 $\times 10^5$ MPa, and the Poisson's ratio is 0.3. Using Eq. (47) to calculate the distortional buckling critical stress is shown in Table 2. The estimated distortional buckling critical stresses by the ANSYS finite element analysis, the proposed formula (Eq. (47)), the Lau and Hancock' formula (1987) and the Silvestre and Camotim' formula (Silvestre and Camotim 2004, Silvestre and Camotim 2010) are 236.9 MPa, 237.5 MPa, 240.9 MPa and 241.0MPa respectively. A comparison with the estimated stress by the ANSYS finite element analysis shows that the error is 0.3% for Eq. (47), 1.7% for Lau and Hancock' formula, and 1.7% for Silvestre and Camotim' formula.

Table 2 Comparison of distortional buckling stresses under axial compression

Parameters	Results	Parameters	Results	Parameters	Results
α_0/N	4870.0	α_1/mm^2	8.462	α_2/mm^2	-1087.6
α_3 /(N·mm^2)	8.59 ×108	α_4 /(N^2·mm^2)	-3.39 ×1013	η_1 /(N·mm)	1.61 ×106
η_2/N	7.43 ×105	η_3 /(N·mm^2)	4.91 ×107	H_4 /mm^2	1087.9
σ_{PR}/MPa	442.93				

6. Conclusions

By analyzing the elastic distortional buckling of the web subjected to uniform compressive stresses, this study has carried out a thorough investigation on the rotational restraint stiffness of the lipped flange. A simplified explicit expression for the rotational restraint stiffness of the lipped flange has then been derived. Based on the explicit expression of the rotational restraint stiffness developed in this study and the approximate distortional buckling model developed by Lau and Hancock (1987), a simplified analytical formula has been derived, which can determine the elastic distortional buckling critical stress of CFLCCs subjected to axial compression. Based on the numerical results obtained from both the analytical solutions and the ANSYS finite element analysis, the conclusions are as follows:

(1) A linear coupling relationship exists between the applied forces and the torsional restraint stiffness of the lipped flange, i.e. the rotational restraint stiffness of the lipped flange can be determined not only from the geometry and material characteristics of a CFLCC but also from the applied forces.

(2) The torsional restraint stiffness of the lipped flange is positive when the applied stress σ is less than the critical stress σ_0. On the other hand, it is negative when the applied stress σ is greater than σ_0, and equals to zero when the applied stress σ equals to σ_0.

(3) The developed analytical formula for the distortional buckling critical stress of the CFLCCs is easy to use with manual calculations, provides a more accurate estimate than the formulas developed by Lau and Hancock (1987). It can be directly used in practical design and incorporated into future design codes and guidelines.

Acknowledgments

The research described in this paper was financially supported by the National Natural Science Foundation of China (51408449, 51378502), the Innovation-driven Plan in Central South University under grant (2015CX006), and the Fundamental Research Funds for the Central Universities of Central South University (2016zzts078), the Special Fund of Strategic Leader in Central South University under grant (2016CSU001).

References

AS/NZS (1996), Cold-formed steel structures; Sydney, Australia.

Benselama, K., El Meiche, N., Bedia, E.A.A. and Tounsi, A. (2015), "Buckling analysis in hybrid cross-ply composite laminates on elastic foundation using the two variable refined plate theory", *Struct. Eng. Mech., Int. J.*, **55**(1), 47-64.

Dar, M.A., Yusuf, M., Dar, A.R. and Raju, J. (2015), "Experimental study on innovative sections for cold formed steel beams", *Steel Compos. Struct., Int. J.*, **19**(6), 1599-1610.

Hancock, G.J. (1997), "Design for Distortional Buckling of Flexural Members", *Thin-Wall. Struct.*, **27**(1), 3-12.

Hancock, G.J., Kwon, Y.B. and Bernard, E.S. (1994), "Strength design curves for thin-walled sections undergoing distortional buckling", *J. Constr. Steel Res.*, **31**(2), 169-186.

He, Z. and Zhou, X. (2014), "Strength design curves and an effective width formula for cold-formed steel columns with distortional buckling", *Thin-Wall. Struct.*, **79**, 62-70.

Jiang, L., Qi, J., Scanlon, A. and Sun, L. (2013), "Distortional and local buckling of steel-concrete composite box-beam", *Steel Compos. Struct., Int. J.*, **14**(3), 243-265.

Kesti, J. and Davies, J.M. (1999), "Local and distortional buckling of thin-walled short columns", *Thin-Wall. Struct.*, **34**(2), 115-134.

Kwon, Y.B. and Hancock, G.J. (1992), "Tests of cold-formed channels with local and distortional buckling", *J. Struct. Eng.-ASCE.*, **118**(7), 1786-1803.

Kwon, Y.B., Kim, G.D. and Kwon, I.K. (2014), "Compression tests of cold-formed channel sections with perforations in the web", *Steel Compos. Struct., Int. J.*, **16**(6), 657-679.

Landesmann, A. and Camotim, D. (2013), "On the Direct Strength Method (DSM) design of cold-formed steel columns against distortional failure", *Thin-Wall. Struct.*, **67**, 168-187.

Landesmann, A. and Camotim, D. (2016), "Distortional failure and DSM design of cold-formed steel lipped channel beams under elevated temperatures", *Thin-Wall. Struct.*, **98**, 75-93.

Lau, S.C.W. and Hancock, G.J. (1987), "Distortional buckling formulas for channel columns", *J. Struct. Eng.-ASCE.*, **113**(5), 1063-1078.

Li, L. and Chen, J. (2008), "An analytical model for analysing distortional buckling of cold-formed steel sections", *Thin-Wall. Struct.*, **46**(12), 1430-1436.

Magnucki, K., Jasion, P., Szyc, W. and Smyczynski, M.J. (2014), "Strength and buckling of a sandwich beam with thin binding layers between faces and a metal foam core", *Steel Compos. Struct., Int. J.*, **16**(3), 325-337.

NAS (2007), North American specification for the design of cold-formed steel structural members (AISI-S100-07), Washington, USA.

Niu, S., Rasmussen, K.J.R. and Fan, F. (2014a), "Distortional-global interaction buckling of stainless steel C-beams: Part I - Experimental investigation", *J. Constr. Steel Res.*, **96**, 127-139.

Niu, S., Rasmussen, K.J.R. and Fan, F. (2014b), "Distortional-global interaction buckling of stainless steel C-beams: Part II - Numerical study and design", *J. Constr. Steel Res.*, **96**, 40-53.

Papangelis, J.P. and Hancock, G.J. (1998), *THIN-WALL*, Sydney Univeisity, Sydney, Australia.

Schafer, B.W. (2012), CUFSM4.05-finite strip buckling analysis of thin-walled members; Johns Hopkins University, Baltimore, USA.

Schafer, B.W. and Peköz, T. (1999), "Laterally braced cold-formed steel flexural members with edge stiffened flanges", *J. Struct. Eng.-ASCE.*, **125**(2), 118-127.

Shenggang, F., Yuelin, T., Baofeng, Z. and Fang, L. (2014), "Capacity of stainless steel lipped C-section stub column under axial compression", *J. Constr. Steel Res.*, **103**, 251-263.

Silvestre, N. and Camotim, D. (2004), "Distortional buckling formulae for cold-formed steel C and Z-section members Part I-derivation", *Thin-Wall. Struct.*, **42**(11), 1567-1597.

Silvestre, N. and Camotim, D. (2004), "Distortional buckling formulae for cold-formed steel C- and Z-section members Part II-Validation and application", *Thin-Wall. Struct.*, **42**(11), 1599-1629.

Silvestre, N. and Camotim, D. (2010), "On the mechanics of distortion in thin-walled open sections", *Thin-Wall. Struct.*, **48**(7), 469-481.

Silvestre, N., Camotim, D. and Dinis, P.B. (2009), "Direct strength prediction of lipped channel columns experiencing local-plate/distortional interaction", *Adv. Steel Constr.*, **5**(1), 49-71.

Teng, J.G., Yao, J. and Zhao, Y. (2003), "Distortional buckling of channel beam-columns", *Thin-Wall. Struct.*, **41**(7), 595-617.

Timoshenko, S.P. and Gere, J.M. (1961), *Theory of Elastic Stability*, McGraw-Hill Book Co., New York, NY, USA.

Tong, G., Feng, Y. and Zhang, L. (2015), "A unified analysis for distortional and lateral buckling of C-purlins in flexure", *Thin-Wall. Struct.*, **95**, 244-254.

Yao, J. (2008), "Distortional buckling loads of cold-formed lipped channels", *Eng. Mechnics.*, **25**(12), 30-34.

Ye, J. and Chen, W. (2013), "Elastic restrained distortional buckling of steel-concrete composite beams based on elastically supported column method", *Int. J. Struct. Stabil. Dyn.*, **13**(1), 1-29.

Young, B., Silvestre, N. and Camotim, D. (2013), "Cold-formed steel lipped channel columns influenced by local-distortional interaction: Strength and DSM design", *J. Struct. Eng.*, **139**(6), 1059-1074.

Yu, C. and Schafer, B.W. (2006), "Distortional buckling tests on cold-formed steel beams", *J. Struct. Eng.-ASCE.*, **132**(4), 515-528.

Zhou, W., Li, S., Huang, Z. and Jiang, L. (2016a), "Distortional buckling of I-steel concrete composite beams in negative moment area", *Steel Compos. Struct., Int. J.*, **20**(1), 57-70.

Zhou, W., Li, S., Jiang, L. and Huang, Z. (2015a), "Distortional buckling calculation method of steel-concrete composite box beam in negative moment area", *Steel Compos. Struct., Int. J.*, **19**(5), 1203-1219.

Zhou, X., Liu, Z. and He, Z. (2015b), "General distortional buckling formulae for both fixed-ended and pinned-ended C-section columns", *Thin-Wall. Struct.*, **94**, 603-611.

Zhou, W., Jiang, L., Li, S. and Kong, F. (2016b), "Elastic distortional buckling analysis of I-steel concrete composite beam considering shear deformation", *Int. J. Struct. Stab. Dyn.*, **16**(8), 1-22.

CC